




# A Combined Strategy to Improve Operational Efficiency of Microgrids with High Integration of Solar and Wind Energy

H. V. P. Nguyen\*<sup>†</sup>, V. T. Nguyen\*, V. H. Nguyen\*

\*Faculty of Electrical Engineering, University of Science and Technology – The University of Danang,  
54 Nguyen Luong Bang, Lien Chieu, Danang, Vietnam

(nhvphuong@dut.udn.vn, tan78dhubk@dut.udn.vn, 105180021@sv1.dut.udn.vn)

<sup>†</sup> Corresponding Author: H.V.P. Nguyen, University of Science and Technology – The University of Danang,  
54 Nguyen Luong Bang, Lien Chieu, Danang, Vietnam.

Tel: +84 917 981 779, nhvphuong@dut.udn.vn

*Received: 06.05.2023 Accepted:06.06.2023*

**Abstract-** Renewable energies offer many benefits in reducing the harm and consequences caused by conventional resources such as fossil fuels. However, the high penetration of renewable energy sources presents a challenge for the operation and stabilization of system frequencies because of the uncertainties of weather factors. Moreover, the renewable energy operation does not participate in the process of supporting the inertia of whole system. Therefore, the paper proposes a combined strategy including storage system and deloading operation to support system frequencies in microgrids to improve operational efficiency. By creating an additional amount of reserve capacity to mobilize in time in case of an imbalance of power, thereby helping to stabilize the frequency. The proposed strategy allows the power grid operation more flexible in such a way that it can appropriately choose either deloading-control or utilizing energy storage sources to support the grid's frequency taking into account the operational conditions. The proposed suggestion has been evaluated in Matlab/Simulink software in multiple cases to show its effectiveness.

**Keywords-** Photovoltaic, wind energy, microgrid, deloading control, frequency control, grid inertia.

## 1. Introduction

Along with the increase in the share of renewable energy resources (RESs), electrical power produced from Photovoltaic Power Plants (PVPPs) and wind turbines (WTs), increasingly affects the stability and control of the power system [1], especially frequency stabilization. The operating principles and inherent characteristics of PVPPs and WTs are the main causes of these effects. Differently from traditional power plants, the output power of PVPPs and WTs systems is often unstable as their operation depends on weather changes. When these RESs are operated at peak power, they do not have the capacity reserve to maintain frequency control [2]. Moreover, PVPPs do not have rotational components like traditional sources, and hence no inertial feedback can be

provided during power imbalance [3]. In addition, the increase of RESs in the power system will reduce the number of traditional generation sources thereby reducing the whole system inertia [4]. This impact becomes more noticeable when they are operated in a standalone system such as Microgrid. The system inertia becomes lower, resulting in a rapid change in the output power of the PVPPs and WTs, which also makes the frequency of the system disturb, deviating from the initial conditions [5]. Therefore, it becomes a challenge to control the system frequency.

Many controlling suggestions for Microgrid operation have been outlined [4], [6]. Several other methods that incorporate RESs sources to support system stability are also mentioned in [7–13]. Especially, some technical methods to support frequencies have given in [4] that are clearly shown in 2 categories: RESs control methods including deloading-

control and inertia response that do not use ESSs; RESs control methods that use ESSs. A summary of specific methods is tabulated in Table 1.

**Table 1.** Inertia and frequency control techniques for RESs

	Without ESSs	With ESSs
PVPPs	Deloading - control	Energy Storage System
WTs	Inertial Response Deloading - control	

In particular, the two most used methods are Energy Storage systems (ESSs) and Deloading-control. These two methods are used due to their popularity and effectiveness in stabilizing the frequency. These suggestions aim to provide additional reserved power capacity to help mitigate power imbalance, thereby stabilizing the system’s frequency. ESSs are a simple and common method to maintain and stabilize the frequency in a system. This helps to keep the frequency stable and minimize the impact of energy fluctuations on the system. They include storage systems and power converters that help provide capacity in an instant when there is a shortage of capacity from the source or consume excess energy to feed into the storage system to help balance the effective capacity. On the other hand, deloading-control is also an effective method to minimize the Rate of Change of Frequency (ROCOF) in a system without relying on Energy Storage Systems (ESSs). It has a separate way of working, instead of operating PVPPs at the Maximum Power Point (MPP), the algorithm operates the system at the point with slightly lower power. Then, PVPPs can maintain a reserved capacity for the system. This reserved amount will be utilized when there is a power imbalance to stabilize the system frequency. However, both methods have several disadvantages: deloading-control gives a better frequency response, but this ability is dependent on weather conditions. Otherwise, the storage system is capable of providing more stable capacity support, but installation and operating costs will increase significantly when a large capacity reserve is required.

To alleviate the disadvantages, this paper proposes a combined strategy of utilizing Energy Storage System and Deloading-control to support microgrid’s frequency. With the proposed combination algorithm, the Deloading-control will minimize the amount of reserve capacity required of the storage system while the Storage System increases the stabilizing capability of the Deloading-control. From there, MG system will operate at a stable frequency, and ensuring power supply reliability. Furthermore, economic efficiency is also enhanced when coordinating the operation of multiple sources such as wind, solar, storage and diesel energy in an islanded MG system [14]. The proposed strategy is evaluated and discussed for frequency support through simulation results using Matlab/Simulink software.

The paper presents the proposed methodology with the following structure: Section 2 describes the frequency response in the power system after a deviation in the power balance. Section 3 in turn specifically demonstrates Storage control and Deloading-control along with supporting

algorithms such as Droop control and ANN algorithm. In section 4, the proposed method of combining the two operating methods is presented in detail according to the operating conditions. Section 5 shows the simulation results and discussion on the proposal. Finally, the review and conclusions are outlined in Section 6.

**2. Microgrid and Overview of Frequency Response in Microgrid Systems**

*2.1. Microgrid System*

*2.1.1. Structure of Microgrid*

According to [15], Microgrid is a group of Distributed Energy Resources (DERs), including Renewable Energy Sources (RESs) and Energy Storage Systems (ESSs), and loads that operate locally as a single controllable entity. Microgrids can be operated at low or medium-voltage levels and in various sizes. They can be large and complex networks, up to tens of MW in capacity, with multiple power resources and storage units serving different loads. Otherwise, microgrids can be small and simple systems, in the range of hundreds of kW, providing electric power to just a few customers.

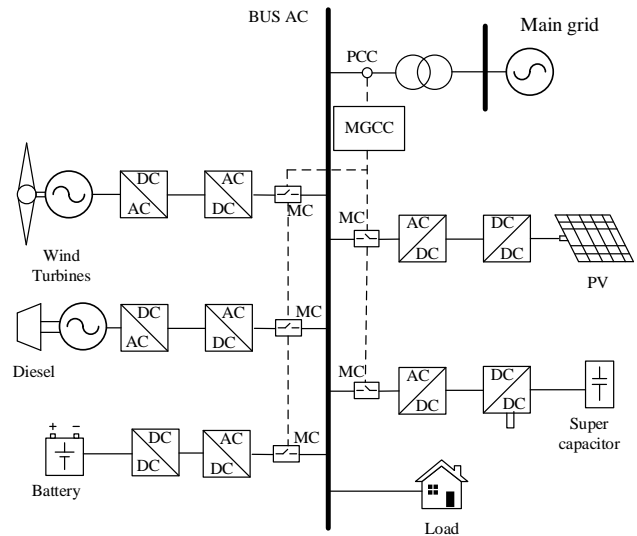


**Fig. 1.** Investigated Microgrid Structure.

The investigated Microgrid structure as shown in Fig. 1 consists of the following components:

- Distributed sources: Wind turbines, solar cells, diesel generators, fuel cells.
- Storage system: Flywheel, supercapacitor, battery.
- Loads.
- Controlling and monitoring systems.

*2.1.2. Frequency Supports of a Microgrid System*

The microgrid has two common operating modes: Island mode and grid-connected mode [16]. With the grid-tied operation, Microgrid functions can be performed through

exchange between MG and the main network. The voltage and frequency of MG at the Point of common coupling (PCC) are mainly determined by the main grid. Each distributed generator element acts as a controllable power source, used to exchange effective and reactive power with the grid, so the ability to support frequencies in the Microgrid is highly dependent on the main grid system.

On the other hand, the Microgrid acts as an independent object separately from the grid in standalone mode. The amount of power generated through MG either actively or passively must be balanced with the amount of power required by the loads. That is, the total output capacity of distributed or storage sources must meet the load capacity demand. The challenge for this mode is that MG had to operate stably on its own so that the frequency value varied within the allowable range. Therefore, the paper focuses on analyzing the frequency response, factors affecting the frequency response process, and proposing frequency support methods for independently operated microgrids.

2.2. Frequency Response Overview

According to [17], the frequency response of the power system consists of three main stages: inertial response (IR), primary frequency response (PFR), and secondary frequency response (SFR) as depicted in Fig. 2. At the IR inertial response stage, the generator speed regulator is adjusted to increase the generator’s output power. In the primary stage, the generators continue to increase the transmitting capacity until the power source and load capacity are equal. To restore the frequency to the nominal value, the frequency control goes through the final stage – the secondary frequency response.

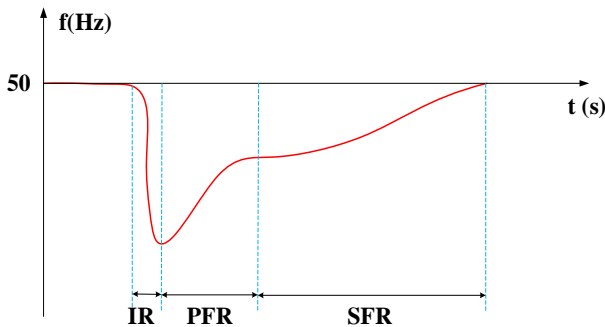


Fig. 2. System frequency response.

The frequency response is dependent on the characteristics of the source. The response time is slow due to the delay time of the speed regulator. Especially in islanded grid systems with high penetration of PVPPs and WTs, the system will significantly reduce the ability to adjust frequencies as traditional energy sources which play an important role in inertial support are minority sources.

2.3. Small Signal Model

To reduce the consequences due to high penetration of RESs, through the proposed strategy to engage frequency support, the system inertia should be increased considerably.

According to [18], the small signal model is illustrated in Fig. 3.

Firstly, the model analyzes the influence of sources on changes in the system’s frequency. From there, the adjusted amount of capacity is determined to balance the power. With different operating methods, using the storage system gives the ability to meet the two-way power capacity corresponding to the ability to charge/discharge instead of just storing and generating capacity like the deloading-control method of PVPPs and WTs.

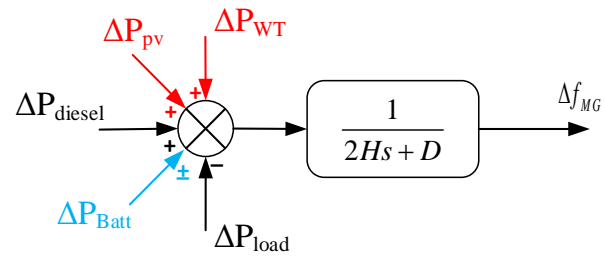


Fig. 3. Small signal model of two proposed methods. (Green: Energy Storage - Red: Deloading-control).

Which:  $\Delta P_{PV}$ ,  $\Delta P_{diesel}$ ,  $\Delta P_{WTs}$ ,  $\Delta P_{ESS}$ , and  $\Delta P_{load}$  are respectively the difference in the effective capacity of PVPPs, diesel generators, WTs, storage, and load systems.

However, systems with many different sources always fluctuate randomly in the system, so frequency stabilization is a difficult issue. Although both methods have the ability to support frequency properly, the reserved capacity is limited. For these reasons, in this paper the power mobilization capabilities are operated according to the droop control method to distribute power accurately and instantaneously between sources capable of moderation in the primary control level, helping to limit the issue just mentioned above.

3. Frequency Support Models of the Two Proposed Strategies

3.1. Storage System

The storage system includes a storage unit for capacity charging/discharging; a power electronic converter; charge/discharge power quantity controller. Batteries are now widely used in standalone power systems due to their relatively low cost and simple operation. Therefore, the paper proposes to use batteries for storage systems.

3.1.1. Equivalent Model of Battery

The equivalent model of battery (BATT) is shown in Fig. 4. According to [19], the BATT output voltage equation is expressed in the following equations:

$$\begin{aligned}
 V &= V_{oc} \pm IR \\
 V_{oc} &= f(SoC) \\
 R &= f(SoC, I, T)
 \end{aligned}
 \tag{1}$$

Where:  $V_{oc}$  is the open-circuit voltage, the voltage will change depending on the state of charge of BATT (SoC);  $R$  is

internal resistance, characterizing internal losses, this value depends on various parameters such as charge/discharge current, temperature and state of charge of BATT; Current  $I$  brings a positive sign during discharging and has a negative sign during charging condition.

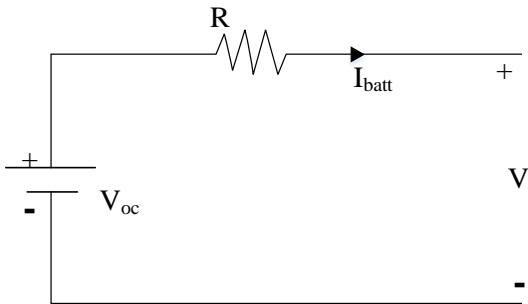


Fig. 4. Equivalent model of BATT.

3.1.2. Bidirectional DC/DC Converter

To perform the task of generating power to the grid and receiving power from the grid, the storage system must be connected to a two-way DC/DC power converter as shown in Fig. 5 [20].

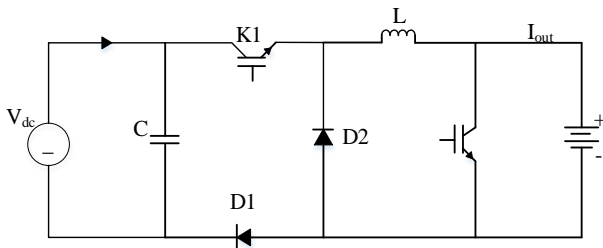


Fig. 5. Bidirectional DC/DC Models.

In charging mode, lock K1 acts as a diode that allows current to enter the storage device. In this mode, the power from the grid will feed into BATT. In contrast, the K1 lock acts as a switch and the K2 lock acts as a diode in discharge mode, the power is transferred from the BATT to the grid to help balance the power between the sources and loads.

3.1.3. Storage System Controller

The main task of the storage system in MG is to generate power in time to help balance the power when fluctuations occur. As the capacity of BATT is limited, it is necessary to incorporate more diesel generators to coordinate the supporting process. The combined Droop Control structure between BATT and Diesel generator is shown as shown in Fig. 6.

The storage system controller consists of a reference current controller and a current controller as shown in Fig. 7. The reference line controller determines the reference current  $d-q$  ( $I_{d-ref}$ ,  $I_{q-ref}$ ) based on the reference power value  $P_{ref}$ ,  $Q_{ref}$ .

By using the error between the reference currents ( $I_{d-ref}$ ,  $I_{q-ref}$ ) and the measured currents ( $I_d$ ,  $I_q$ ), the current controller generates reference voltages  $V_{d-ref}$ ,  $V_{q-ref}$ . Via the  $dq$  frame to

$abc$  frame, the converter feeds a three-phase reference voltage signal to the pulse width modulator (PWM).

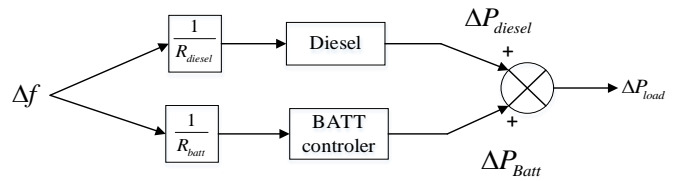


Fig. 6. Combined Battery and Diesel controller structure.

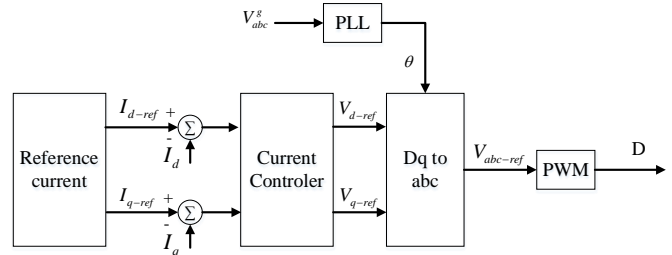


Fig. 7. Battery controller block diagram.

3.1.4. Storage System Control Method

Diesel and Battery Storage Systems work together to maintain Microgrid frequencies stable when there is a change in load and power capacity. The frequency deviation is calculated by the formula:

$$\Delta f = f_{net} - f_{ref} = K_p \Delta P \tag{2}$$

where:  $K_p$  is the characteristic coefficient for the droop characteristic line ( $P-f$ ) and  $\Delta P$  is the deviation of the applied power to be changed of the sources (Diesel and Battery generators).

When the system is operating stably ( $\Delta f=0$ ), the storage system does not discharge nor charge capacity. If there is a fluctuation in frequency, assuming the load increases at this time  $\Delta f < 0$ , the storage system and diesel generator must pump the power to the grid according to the  $P-f$  characteristic line to ensure the balance of load and source. In contrast, when  $\Delta f > 0$  the power of the diesel generator and storage system is adjusted downwards according to  $P-f$  characteristics to balance the load. At this point, BATT will operate in the charge state.

3.2. Power Control Deloading Method

3.2.1. Deloading-control for PVPPs

The offline MPPT algorithm is built from concurrent characteristics and has a faster response speed than other algorithms [21] but the P-V characteristic line is linearized so the power response is less accurate, leading to a decrease in efficiency in frequency support. The Artificial Neural Network (ANN) MPPT algorithm is proposed to limit the shortcomings that exist in other algorithms. Instead of just capturing the Maximum Power Point (MPP), the ANN algorithm builds a family of P-V characteristics according to

environmental conditions characterized by temperature and radiation values, thereby eliminating linearization to increase the accuracy and ability to mobilize power to support the frequency of the system.

In addition, the amount of reserve power will always change because it depends on the radiation value and temperature, so it is proposed to reduce the load for PVPPs using the ANN algorithm combined with the droop control method with a variable droop coefficient to improve the inertia of the system when frequency fluctuations occur.

*a. ANN Algorithm*

An artificial neural network (ANN) is an information processing model that mimics the way biological neural systems process information. It is made up of a large number of elements (called processing elements or neurons) connected through links (called link weighting) that work as a whole to solve a particular problem [22].

ANN is a popular and widely used tool for artificial intelligence modeling. It has strong self-adaptability, fault tolerance and reasoning, so it has been successfully applied to forecasting the capacity of wind farms and solar power plants (PVPPs). ANN can learn complex relationships between outputs and inputs after training [23]. An ANN usually organizes neurons into layers, and each class is responsible for a specific job. ANN usually has a minimum of 3 layers: input layer, hidden layer, and output layer. The structure of a neuron is depicted as shown in Fig. 8.

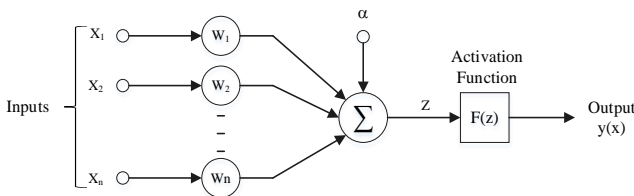


**Fig. 8.** The mathematical structure of an artificial neuron.

The mathematical model of straight propagation ANN is presented as follows:

$$y(x) = f(z) = f\left(\sum_{i=1}^n w_i x_i + \alpha\right) \tag{3}$$

where:

- $y(x)$ : Output value in variable  $x$
- $f(z)$ : Activation function
- $w_i$ : Weighting of  $x_i$  neurons
- $x_i$ : Input values
- $\alpha$ : Correction factor.

Various activation functions are proposed such as tanh, liner and sigmoid functions; In this study using the Sigmoid function in equation (4):

$$y = \frac{1}{1 + e^{-z}} \tag{4}$$

The structure of a multilayer linear propagation ANN considered in the proposed application is depicted in Fig. 9.

The data of photovoltaic solar panels (PV) is calculated. Here, the neurons of the input layers act as buffers to distribute that data as input signals including PV output power ( $P_{PV}$ ) and environmental conditions such as radiation and temperature. The output layer has a neuron that provides  $V_{PV}$  voltage values including Maximum Power Point Voltage ( $V_{MPP}$ ) corresponding to Maximum Power Point Power ( $P_{MPP}$ ) to form a complete characteristic family. The training data was obtained using Matlab/Simulink to simulate the parameters of the PV panels provided by the manufacturer. The paper uses a PVPPs system model using SunPower SPR-30SE-WHT-D/100kW modules with the parameters given in Table 2.

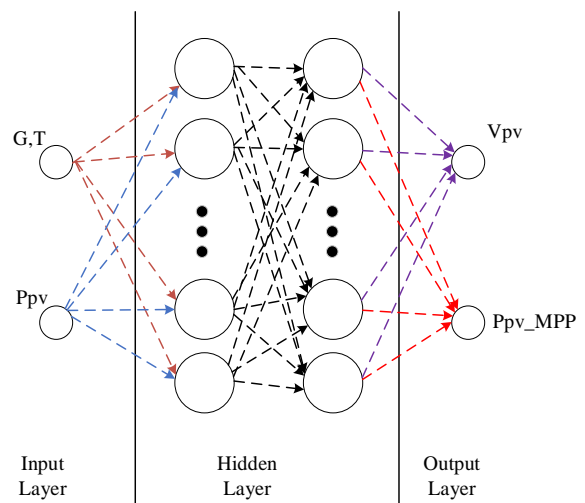


**Fig. 9.** Multilayer relay neural networks.

**Table 2.** Parameters of a PV model panel

Parameters (standard conditions)	Parameter	Value
Maximum power	$P_{MPP}$	305W
Current at MPP point	$I_{MPP}$	5.58A
Voltage at MPP point	$V_{MPP}$	54.7V
Short-circuit current	$I_{sc}$	5.96A
Open-circuit voltage	$V_{oc}$	64.2V
Number of panels connected in series	$N_s$	5
Number of battery arrays in parallel	$N_p$	66

*b. Deloading-control for PVPPs*

Deloading control is a new technique that helps PVPPs reserve an amount of  $\Delta P$  capacity during operation. This portion of the power will not be mobilized until the system has a frequency deviation [4]. Based on the constructed  $P$ - $V$  characteristic curve, instead of operating at  $V_{MPP}$  corresponding to the Maximum Power Point (MPP), PVPPs are operated at a point where the voltage is greater or lower than the voltage at the MPP point [24].



To reserve an amount capacity of  $\Delta P$ , the PVPPs system will be operated at  $P_{deload}$  capacity with a power reserve factor of  $d\%$  [4]. The power generated can be calculated by the formula:

$$P_{deload} = (1 - d)P_{MPP} \tag{5}$$

The operation analysis is depicted in Fig. 10. With efficiency in capturing maximum power points, the ANN algorithm will operate in deloading mode to different environmental conditions regardless of the characteristics of the  $P$ - $V$ . Corresponding to the maximum working point ( $P_{MPP}$ ,  $V_{MPP}$ ), based on the built-characteristic family, PVPPs will be operated at one of two points of the  $P_{deload}$  capacity ( $V_{d1}$  corresponds to the left flank and  $V_{d2}$  corresponds to the right flank of the characteristic line).

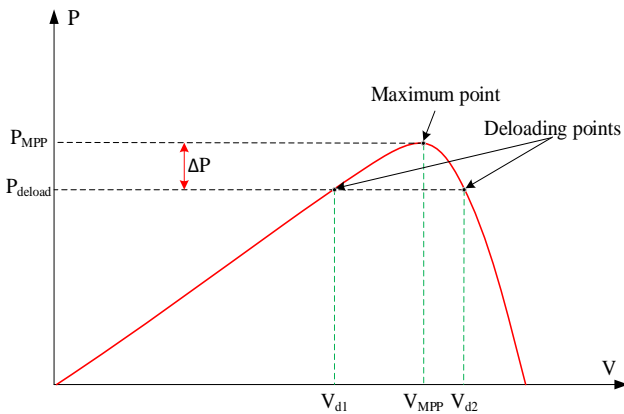


Fig. 10. Deloading operation of PVPPs.

c. Analysis of Energy Reserve in Deloading Mode

The operating temperature of the system is  $T=25^{\circ}\text{C}$  and the change of solar radiation  $G$  is given in Fig. 11. Figure 12 shows the capacity reserve of PVPPs in deloading mode. In particular,  $P_{MPP}$  is the maximum power that the PVPPs system can provide and  $P_{deload}$  is the amount of power that the PVPPs system provides when operating in deloading mode.

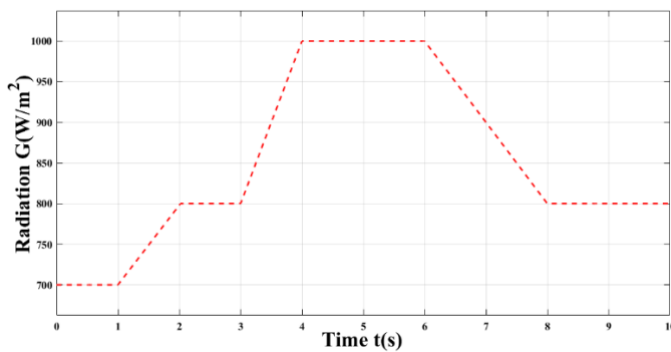


Fig. 11. Variable radiation characteristics.

When PVPPs operate in deloading mode to store energy, along with a certain reserve level  $d\%$ , if the radiation changes, the reserve capacity will also change, the lower the radiation, the smaller the amount of stored power as shown in Fig. 12.

d. Power Mobilization Methods to Support Frequency

With a certain rated power, a conventional diesel generator has a constant droop coefficient. However, with the varied reserve capacity mentioned above due to weather conditions, the droop factor needs to be changed accordingly. Based on the droop-control method in [25], a droop-control method in which droop coefficient varies according to the reserve capacity for PVPPs as follows:

$$\Delta P(f) = \Delta f \times K = \Delta f \times \frac{\Delta P}{R} \tag{6}$$

Where  $R$  is the allowable frequency deviation of the system when there are small fluctuations and  $\Delta P$  is the reserved power of PVPPs corresponding to a specific radiation value and temperature in equation (7):

$$\Delta P(t) = P_{MPP}(t) - P_{Deload}(t) \tag{7}$$

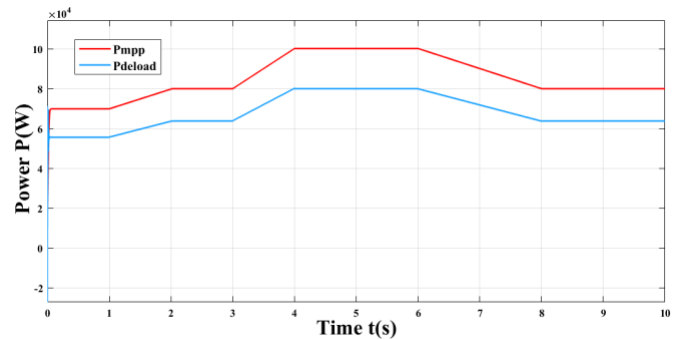


Fig. 12. Generated power when operating at MPPT and Deloading condition.

3.2.2. Power Control According to the Deloading-Control of WTs

With the high penetration rate of wind power, when operating in MPPT power tracking mode, this system will not respond to the frequency change of the grid and lack frequency tuning ability. Therefore, a large number of WTs connected to the grid will reduce frequency stability. To improve the stability of the system frequency, it is necessary to have a control method for the WTs system to be able to respond to changes as well as maintain the stability of the system frequency. The proposed method is to use a deloading operation to create a capacity reserve. This reserved power is delivered to the system when necessary to support the frequency.

a. Deloading-control for WTs

Based on the optimal torque (OT) peak power scoring method introduced in [26], control of the rotor rotation speed of WTs according to the MPPT characteristic line is shown in Fig. 13. WTs power peaks at optimum speed  $\omega_0$ , when increasing or decreasing the rotor speed to  $\omega_1$  and  $\omega_2$ , it is possible to reduce the output power of WTs at the deloading operation point [27]. However, deloading operation by

increasing speed is recommended since reducing speed often causes several stability problems.

*b. Frequency Support via Power Mobilization*

As affected by weather conditions, the power reserve capacity and frequency support of power generation of WTs are relatively similar to PVPPs. Therefore, the method of controlling the droop of WTs is expressed similarly to the equation (6) where  $R$  is the generator droop parameter of WTs. The general diagram of the deloading operation method is shown in Fig. 14.

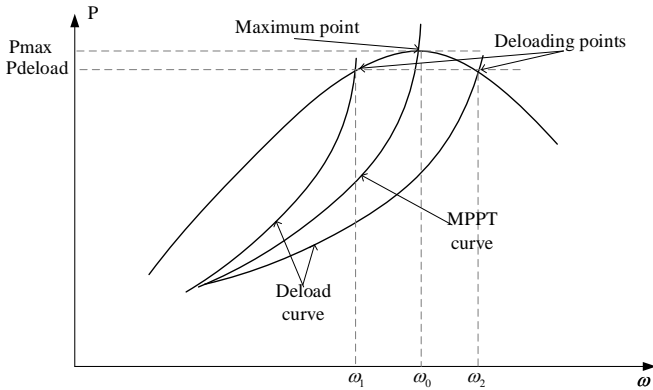


**Fig. 13.** Deloading-control for wind power systems.

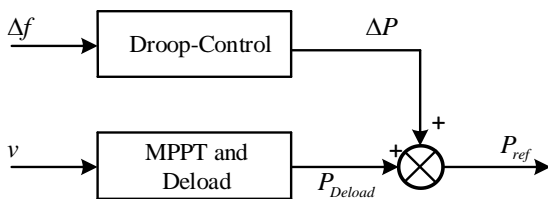


**Fig. 14.** Block diagram of the frequency support of WTs.

When there is a change in frequency, the droop control unit will indicate the amount of power that needs to be mobilized. Hence, it is combined with the deloading power  $P_{deload}$  to create the reference signal power  $P_{ref}$  to transfer to the speed control controllers.

**4. Frequency Support Strategy for Microgrids**

*4.1. Combined Operation Strategy*

During the combined operation of renewable energy sources in the microgrid, environmental and weather conditions have a great impact on operational efficiency. For example, at night or in bad weather, the amount of stored capacity from renewable energy sources is negligible or even nonexistent, leading to the ability to mobilize capacity to stabilize the system frequency at this time is not high, which means that the working reliability has decreased significantly. While the storage method is less affected by weather conditions and provides more stable system support capacity, the operation, maintenance, and installation costs will increase when large capacity reserves are required.

To mitigate the disadvantages of the two methods, the combined method of Energy Storage System and Deloading-control Strategy is proposed to support grid frequency. With this method, the deloading operation will reduce the amount of required reserve capacity of ESSs and at the same time, ESSs help increase the stability of the Deloading operation which is highly dependent on weather conditions. As a result, MG System will operate at a stable frequency, ensuring power supply reliability.

*4.2. Constraints for Developing the Proposed Strategy*

The proposed strategy is built to utilize the advantages of the two methods of Storage and Deloading operation. The boundary conditions help to propose a combination of alleviating the disadvantages, thereby helping the frequency operation of the microgrid system more stable. Requiring conditions are as follows:

- Deloading performance: referred to as the reserve capacity of each renewable source. Depending on specific conditions, the capacity reserve of each source will vary. The purpose of this condition is to provide specific reserves to support system inertia while ensuring the most optimal power supply for each source.
- Weather: For each region, season, or month of the year, weather conditions also changed. This will be a major obstacle to deloading operation when the amount of capacity is always changed. Therefore, the weather factor is one of the conditions that should be kept in mind when building this combined plan.
- Economy: Using storage requires high investment, operation and maintenance costs when having to reserve large capacity. The deloading operation method increases the amount of reserved power that can be generated in the system compared to when the system is working in MPPT [28-29]. The combination method helps reduce the installed capacity of the storage system because PVPPs and WTs can assist in balancing system power from the amount of reserved capacity.
- Technical characteristics: the capacity to reserve and generate power to support the power balance of each source is different. It can be seen most clearly in both wind and solar sources: While in wind sources, turbines suffer a delayed response due to inertia while operating generators and wind turbine structures (gearboxes, couplings, etc.), in solar sources, the response time is faster due to not suffering similar inertia. Therefore, it is necessary to consider this condition to ensure better storage and power generation when combining sources.

*4.3. Algorithm Flowchart of the Proposed Strategy*

From the aforementioned constraints, the proposed algorithm flowchart is shown in Fig. 15.  $PV_{deload}$  is deloading mode of PVPPs and  $WT_{deload}$  is wind turbine deloading mode.

Two characteristic quantities of solar energy and wind energy sources are used to facilitate the algorithm. The radiation parameter of  $G_o$  and the wind velocity of  $v_o$  are

determined condition for each operating mode. When  $G > G_o$  and  $v > v_o$ , PVPPs and WTs will operate in the deloading method. When  $G \leq G_o$  or  $v \leq v_o$ , PVPPs or WTs will operate respectively at MPPT conditions, and the storage system is standby to generate power to the grid when there is a frequency deviation.

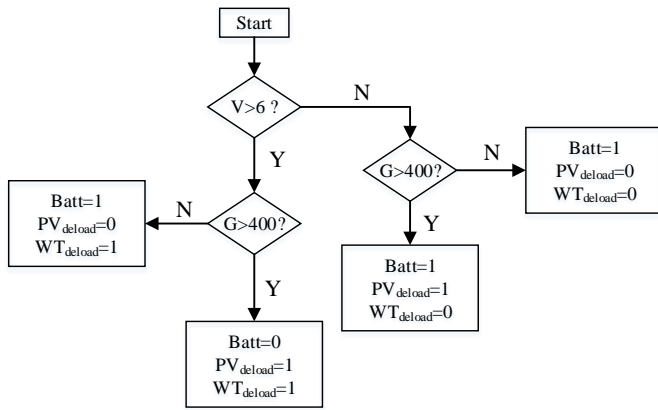


Fig. 15. Algorithmic flowchart of the proposed strategy.

4.4. Survey of Operating Conditions for Algorithmic Flowcharts

To select appropriate values  $v_o$  and  $G_o$ , it is necessary to take into account the boundary constraints already stated. With specific investigated conditions, the desired values are set in the proposed algorithm flowchart. Based on Matlab/Simulink software, models of PVPPs and WTs systems of 2MW are carried out to obtain the amount of generated capacity according to introduced conditions. The results in Table 3 and 4 respectively show the exploitable capacity value and the amount of stored capacity of PVPPs and WTs corresponding to different radiation values and wind speeds.

Table 3. Estimated reserves for each wind speed

Wind velocity [m/s]	$P_{mppt}$ [MW]	$\Delta P$ [kW]
10	1.357	135.735
9.5	1.164	116.376
9	0.990	98.951
8.5	0.834	83.358
8	0.695	69.496
7.5	0.573	57.263
7	0.466	46.557
6.5	0.373	37.276
6	0.293	29.319
5.5	0.226	22.583
5	0.170	16.967
4.5	0.124	12.369

Table 4. Estimated reserved capacity for each radiation

Radiation [W/m <sup>2</sup> ]	$P_{mppt}$ [kW]	$\Delta P$ [kW]
1000	300.965	60.193
900	270.746	54.149
800	240.428	48.086
700	210.031	42.006
600	179.577	35.915
500	149.097	29.819
400	118.633	23.727
300	88.251	17.650
200	58.058	11.612
100	28.283	5.657

Corresponding to wind speed of 6 m/s and solar radiation of 400 W/m<sup>2</sup>, the power reserve of PVPPs and WTs at this instant is relatively low, so the support capacity is negligible. Therefore, in this paper, two conditional variables are set at  $v_o = 6$  m/s and  $G_o = 400$  W/m<sup>2</sup> for the algorithmic flowchart to conduct the simulations in section 5.

5. Simulations

The paper simulates and evaluates the effectiveness of the proposed algorithm in the frequency stability of the microgrid system. Supposedly, the system change in power capacity is caused by two main reasons:

- Due to the variability of the load
- Due to the change of generated power from the WTs depending on the wind velocity.

The overview structure of the simulated microgrid is shown in Fig. 16. For each scenario, a comparison of simulation results in 2 different operating cases is evaluated: operating PVPPs and WTs at maximum capacity with combining ESS (Case 1) and operating according to the proposed algorithm (Case 2).

In this investigated islanded system, the standalone grid consists of PVPPs, WTs, ESS, and a diesel generator as electrical sources. The nominal power ratings of the sources are shown in Fig. 16. These ratings are empirically given to similarly behave as a power grid of an island without connected to the utility. The values of sources are reasonable to validate the effectiveness of the proposed algorithm.

5.1. Simulation Results

5.1.1. Scenario 1: Power Remains Constant, Load Changes

In the first scenario, the load capacity initiates at 3.14MW, from the 5<sup>th</sup> second the load increases by 170kW to the 5.2<sup>th</sup> second, the load reaches 3.31MW and keeps at this level.



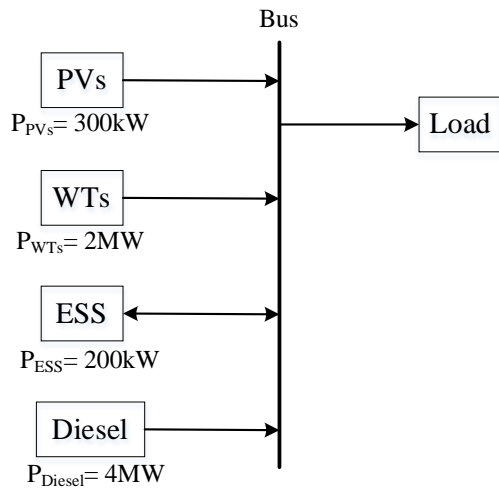


**Fig. 16.** Standalone Microgrid Overview Structure.

Figure 17 shows the ability to mobilize power capacity according to the load power in each case.

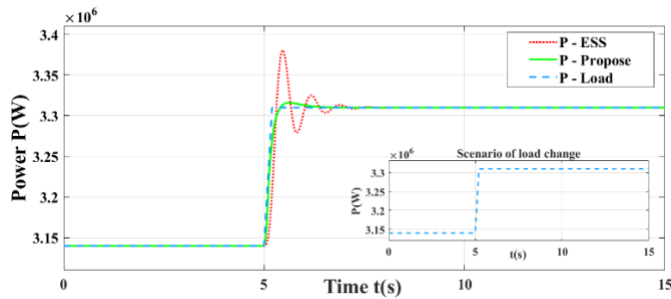


**Fig. 17.** Capacity response when load changes.

Where the system operates in MPPT, the Diesel and ESS generators are two components that take care of the power balance between power and load. However, both components need time to increase the amount of power to be mobilized, so the fluctuation in power capacity at this time is very large. In case 2, the operation according to the proposed algorithm allows the system to mobilize power quickly from the reserved capacity, the remaining shortage is fulfilled by the Diesel generator. The amount power compensated from Diesel is not much, so allowing the system to mobilize power quickly resulting in a significantly reduced power fluctuation compared to the case of operating in MPPT.

Figure 18 shows the amount of power mobilized from each source when the system operates according to the proposed algorithm. When the load increases, PVPPs and WTs mobilize the reserved capacity according to the reserve coefficient  $d\%$  of each source ( $d_{PVPPs} = 20\%$ ,  $d_{WTs} = 10\%$ ), the diesel generator adjusts to increase the capacity to compensate for the lack of capacity to balance the power capacity with the load capacity. The power mobilization rate is also clearly shown in Fig. 18, PVPPs and WTs can quickly mobilize the reserved power in deloading mode whereas the Diesel generator needs more time to adjust the generated power. When PVPPs mobilize close to the maximum reserved capacity (about 60kW) and reach the steady state, the total mobilized capacity of all three sources of PVPPs, WTs and Diesel are higher than the amount of power needed

to balance the load, so PVPPs begins to reduce the amount of mobilized power due to faster adjustment time than Diesel.

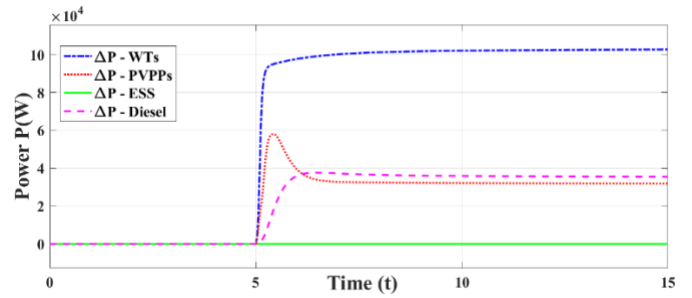


**Fig. 18.** Respond to the capacity of each source with the proposed algorithm.

This reaction explains why the mobilization capacity of PVPPs is set below the maximum value. The proposed algorithm only allows ESS to assist the system frequency when either wind velocity or solar radiation or both values are below the limit. In this scenario, the wind velocity at 9.03m/s and solar radiation at 1000W/m<sup>2</sup> are constant and above the limit, so the ESS does not work.

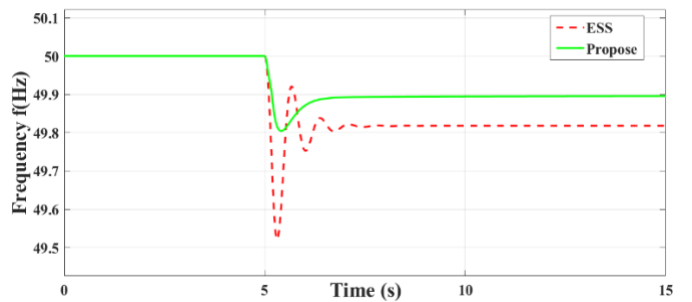


**Fig. 19.** Frequency feedback when load changes.

The capacity mobilization of two cases results in the corresponding frequency response shown in Fig. 19. In the case that MPPT operation incorporates with ESS, the system frequency fluctuates a lot and falls below the permissible limit (about 49.52 Hz). The transient time to reach the steady state is quite long (about 3s) and the frequency after fluctuation is low (about 49.82 Hz). On the contrary, the system frequency oscillates within the allowed range in the case of operation according to the proposed algorithm (about 49.81Hz), and the transient time to achieve the steady state is relatively quick (about 2s) and the frequency after the fluctuation is significantly enhanced (about 49.90 Hz).

*5.1.2. Scenario 2: Constant Load, Variable Wind Velocity*

In scenario 2, the power capacity changes due to a decrease in wind velocity from 7m/s to 6m/s at the 5th second. Fig. 20 shows the mobilization capacity of two operating cases. When a decrease in wind velocity causes a power imbalance ( $P_{power} < P_{load}$ ), an additional amount of generated power is needed to support the system frequency. Like scenario 1, this amount of power is to be compensated for by the Diesel generator and ESS because the MPPT operating system incorporates ESS. Hence, the power fluctuation in the system is very large and the time to reach

the reference value is relatively long. Power fluctuations have been significantly improved when the system operates according to the proposed algorithm, and the time to reach the stable state is also faster.

Figure 21 shows the amount of power mobilized from sources when the system operates according to the proposed algorithm. When the wind speed is less than or equal to 6m/s, the amount of power forecast is negligible. Therefore, the WT's system switches to MPPT operating mode and the ESS is utilized to support power balance. From 5s to 5.2s, the wind speed starts decreasing. During this period, the wind speed is still greater than 6m/s, so WT's are still working in deload mode with  $\Delta P_{WTs} > 0$ . From the 5.2s onwards, the wind speed is 6m/s, WT's work at MPPT condition so the power reserve is now zero. PVPPs are still working in deload mode, so it will generate the reserved power in combination with ESSs and diesel generators to support the system frequency. The power mobilization rate is also shown in Fig. 21. PVPPs working in deload mode can quickly mobilize the reserve power while Diesel generators and ESSs need more time to adjust the generating power. When PVPPs mobilize to the maximum reserve power (about 48kW corresponding to 800 W/m<sup>2</sup> radiation) and reach the steady state, the total mobilized capacity of all three sources PVPPs, ESS and Diesel are higher than the needed amount of power to be mobilized to balance the load capacity, so PVPPs and ESS adjust to reduce the amount of mobilized power due to the adjustment time of these two sources are faster than that of Diesel. This explains the fact that the mobilization capacity of PVPPs is below the maximum level and the mobilized capacity of ESS starts to decrease when the mobilized capacity from the diesel generator is established.

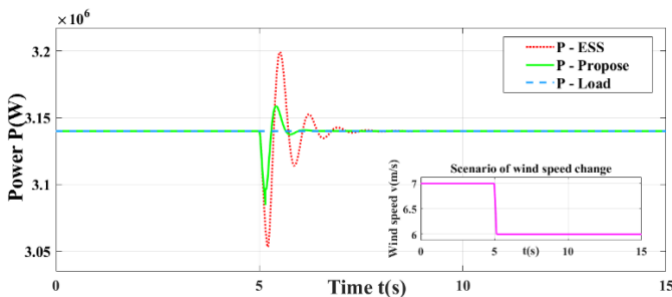


Fig. 20. Capacity response when wind speed changes.

The capacity mobilization of two cases resulting in the corresponding frequency response is shown in Fig. 22. In the case of MPPT operation combined with ESS, the system frequency fluctuates a lot and is outside the permissible limit (about 49.57 Hz), the time to reach the stable state is long (about 3s) and the frequency after the fluctuation is quite low (about 49.82Hz). On the other hand, the system frequency oscillates within the allowed range in the case of operating the proposed algorithm (about 49.81Hz), the time to reach the reference is faster (about 1.5s) and the frequency after the fluctuation is significantly enhanced (about 49.89Hz).

5.2. Discussion

The proposed combined frequency support strategy for Energy Storage System and Deloading-control shows good

responsiveness in some of the cases investigated. Strategically operated cases with the proposed method get better results than in cases operating in a conventional way of operating in MPPT or supported solely by a battery storage system. The combined strategy promotes the advantages of the Energy Storage System and deloading-control operation methods, thereby compensating for the shortcomings of the other algorithm. Hence, the stability of RESs is enhanced, and improving stability and reliability in MG systems.

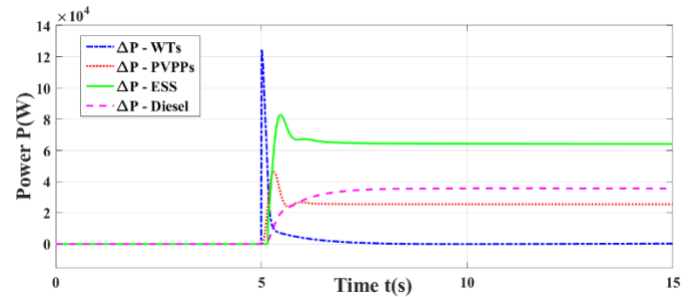


Fig. 21. The capacity response of each source with the proposed algorithm when wind speed changes

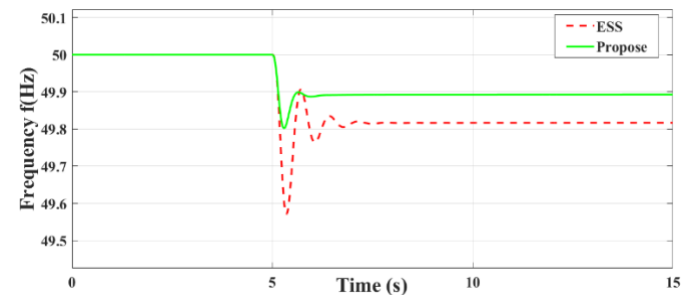


Fig. 22. Frequency feedback when wind speed changes.

For deloading operation, reserved output power can help renewable sources expand in size and output while regulating the penetration of these sources into the power system. Due to the utilization of a part of the power capacity from the deloading operation, the initial investment cost in the storage system is reduced, and thus increasing economic efficiency.

By utilizing a combination proposal for existing algorithms and methods, their operational flexibility can be increased. This ensures the optimal operability of each method while giving it the ability to combine two or more different methods to get the most out of the support supply or manage multiple sources comprehensively to maintain the system's frequency support.

The combination proposal can bring several benefits. Instead of relying on a single methodology, a flexible strategy can be adopted, depending on the specific operating condition of system changes. This ensures that the most appropriate method is utilized in all cases, and thus achieving the highest efficiency. Moreover, combining different control methods can utilize various types of generated sources including RESs to maintain the system's frequency. Instead of relying on a single source, multiple sources can be combined to ensure continuity and reliability during operation. This is especially useful in frequency support

systems, where managing and utilizing multiple inconsistent sources such as solar and wind energy are important to ensure stability and efficiency.

However, the proposed strategy does not fully show the process of Frequency Response in the system (section 2.1) including the secondary response phase. Thus, it is not possible to bring the frequency to the nominal value after the transient state. Therefore, simulation scenarios are not performed in complex cases such as changes of power and load values within a day.

## 6. Conclusion

The paper proposes an operational strategy to support frequencies in microgrids with high penetration of renewable energy by combining deloading control and Storage systems. The combined proposal makes some contributions to the general development in system frequency stabilization. The paper suggests some new utilizations such as ANN and good use of droop control algorithm to optimize desired results. From the simulation results, the system frequency is well responded to when deloading operation for each specific scenario. In addition, the storage system has also contributed effectively to the capacity balance whenever renewable energy sources work in bad weather conditions – there is no amount of stored capacity. As a result, the stability, efficiency and reliability of microgrids have been significantly enhanced. This proposal is worth considering when operating and developing the power grid with the penetration of RESs. However, the current flowchart is still flawed and does not adequately respond to the situation in practice. This leads to the impossibility of simulating special scenarios that may occur during operation. Therefore, the future direction of development is to consider other aspects to meet the actual operation of the grid with high penetration of RESs.

## Nomenclature

Abbreviation	Description
ANN	Artificial Neural Network
BATT	Battery
DERs	Distributed Energy Resources
ESSs	Energy Storage Systems
IR	Inertial Response
MG	MicroGrid
MPP	Maximum Power Point
MPPT	Maximum Power Point Tracking
PFR	Primary Frequency Response
PVPPs	Photovoltaic Power Plants
PWM	Pulse Width Modulator
RESs	Renewable Energy Resources
ROCOF	Rate of Change of Frequency
SFR	Secondary Frequency Response
WTs	Wind Turbines

Symbol	Description
$I_{sc}$	Short-circuit current
$I_{MPP}$	Current at MPP point
$G$	Radiation
$P_{deload}$	Power when operation deloading-control
$P_{MPP}$	Maximum power
$T$	Temperature
$V_{oc}$	Open-circuit voltage
$V_{MPP}$	Voltage at MPP point
$v$	wind velocity

## Acknowledgements

This work was supported by The University of Danang, University of Science and Technology, code number of Project: T2022-02-10.

## References

- [1] T. Meridji, G. Joós, and J. Restrepo, “A power system stability assessment framework using machine-learning”, *Electric Power Systems Research*, vol. 216, 2023.
- [2] P. P. Zarina, S. Mishra, and P. C. and Sekhar, “Photovoltaic system based transient mitigation and frequency regulation”, *2012 Annual IEEE India Conference (INDICON), Kochi, India*, IEEE, pp. 1245–1249, 2012.
- [3] Y. T. Tan and D. S. Kirschen, “Impact on the power system of a large penetration of photovoltaic generation”, *2007 IEEE Power Engineering Society General Meeting, Tampa, FL, USA*, pp. 1–8, 2007.
- [4] M. Dreidy, H. Mokhlis, and Saad Mekhilef, “Inertia response and frequency control techniques for renewable energy sources: A review”, *Renewable and Sustainable Energy Reviews*, vol. 69, pp. 144–155, 2016.
- [5] M. Farrokhabadi, C. A. Cañizares, and K. Bhattacharya, “Frequency control in isolated/islanded microgrids through voltage regulation”, *IEEE Trans Smart Grid*, vol. 8, no. 3, pp. 1185–1194, 2017.
- [6] G. Delille, B. Francois, and G. Malarange, “Dynamic frequency control support by energy storage to reduce the impact of wind and solar generation on isolated power system’s inertia”, *IEEE Trans Sustain Energy*, vol. 3, no. 4, pp. 931–939, 2012.
- [7] K. Paul, “Modified grey wolf optimization approach for power system transmission line congestion management based on the influence of solar photovoltaic system”, *International Journal of Energy and Environmental Engineering*, vol. 13, no. 2, pp. 751–767, 2022.
- [8] K. Paul, “Multi-objective risk-based optimal power system operation with renewable energy resources and

- battery energy storage system: A novel Hybrid Modified Grey Wolf Optimization–Sine Cosine Algorithm approach”, *Transactions of the Institute of Measurement and Control*, 2022.
- [9] K. Paul and N. Kumar, “Cuckoo search algorithm for congestion alleviation with incorporation of wind farm.”, *International Journal of Electrical & Computer Engineering (2088-8708)*, vol. 8, no. 6, 2018.
- [10] K. Paul, P. Dalapati, and N. Kumar, “Optimal rescheduling of generators to alleviate congestion in transmission system: A novel modified whale optimization approach”, *Arab J Sci Eng*, vol. 47, no. 3, pp. 3255–3279, 2022.
- [11] M. Maaruf, S. El Ferik, F. S. Al-Ismail, and M. Khalid, “Robust Optimal Virtual Inertia Control for Microgrid Frequency Regulation Considering High Renewable Energy Penetration”, *2022 11th International Conference on Renewable Energy Research and Application (ICRERA)*, pp. 369–373, 2012.
- [12] S. Esmer and E. Bekiroglu, “Design of PMaSynRM for Flywheel Energy Storage System in Smart Grids”, *International Journal of Smart Grid-ijSmartGrid*, vol. 6, no. 4, pp. 84–91, 2022.
- [13] M. Allouche, S. Abderrahim, H.B. Zina, and M. Chaabane, “A Novel fuzzy Control Strategy for Maximum Power Point Tracking of Wind Energy Conversion System”, *International Journal of Smart Grid-ijSmartGrid*, vol. 3, no. 3, pp. 120–127, 2019.
- [14] W. Su, Z. Yuan, and M.-Y. Chow, “Microgrid planning and operation: Solar energy and wind energy”, *IEEE PES General Meeting*, IEEE, pp. 1–7, 2010.
- [15] M. Farrokhhabadi, C.A. Canizares, J.W.Simpson-Porco, E. Nasr, L. Fan, P.A. Mendoza-Araya, R. Tonkoski, U. Tamrakar, N. Hatzigiargyriou, D. Lagos, R.W. Wies, M. Paolone, M. Liserre, L. Meegahapola, M. Kabalan, A.H. Hajimiragha, D. Peralta, M.A. Elizondo, K.P. Schneider, F.K. Tuffner, and J. Reilly, “Microgrid stability definitions, analysis, and examples”, *IEEE Transactions on Power Systems*, vol. 35, no. 1, p. 13, Jan. 2020.
- [16] L. O. Mogaka, G. N. Nyakoe, and M. J. Saulo, “Islanded and Grid-Connected Control in a Microgrid with Wind-PV Hybrid”, *International Journal of Applied Engineering Research*, vol. 15, no. 4, pp. 352–357, 2020.
- [17] C. Rahmann and A. Castillo, “Fast frequency response capability of photovoltaic power plants: The necessity of new grid requirements and definitions”, *Energies (Basel)*, vol. 7, no. 10, pp. 6306–6322, 2014.
- [18] N.H. Hieu, N.V. Tan, N.B. Nam, T.D.M. Duc, D.H. Dan, and L.Q. Cuong, “The roles of energy storage systems in stabilizing frequency of the islanded microgrid”, *Journal of Science and Technology – The University of Danang*, vol. 18, no. 5.2, pp. 39–44, 2020.
- [19] N. Achaibou, M. Haddadi, and A. Malek, “Modeling of lead acid batteries in PV systems”, *Energy Procedia*, vol. 18, pp. 538–544, 2012.
- [20] B.Y. Li, C. Xu, C. Lib, and Z. Guan, “Working principle analysis and control algorithm for bidirectional DC/DC converter.”, *Journal of Power Technologies*, vol. 97, no. 4, 2017.
- [21] S. Malathy and R. Ramaprabha, “Maximum power point tracking based on look up table approach”, *Advanced Materials Research*, vol. 768, Trans Tech Publications, pp. 124–130, Sept. 2013.
- [22] A. Abraham, “Artificial Neural Networks”, *Handbook of Measuring System Design*, Jul. 2005.
- [23] H. Zhu, X. Li, Q. Sun, L. Nie, J. Yao, and G. Zhao, “A power prediction method for photovoltaic power plant based on wavelet decomposition and artificial neural networks”, *Energies (Basel)*, vol. 9, no. 1, p. 11, 2015.
- [24] R. Rajan, F. M. Fernandez, and Y. Yang, “Primary frequency control techniques for large-scale PV-integrated power systems: A review”, *Renewable and Sustainable Energy Reviews*, vol. 144, p. 110998, 2021.
- [25] U. B. Tayab, M. A. Bin Roslan, L. J. Hwai, and M. Kashif, “A review of droop control techniques for microgrid”, *Renewable and Sustainable Energy Reviews*, vol. 76, pp. 717–727, 2017.
- [26] J. Pande, P. Nasikkar, K. Kotecha, and V. Varadarajan, “A review of maximum power point tracking algorithms for wind energy conversion systems”, *J Mar Sci Eng*, vol. 9, no. 11, p. 1187, 2021.
- [27] X. Zhang, Y. Chen, Y. Wang, X. Zha, S. Yue, X. Cheng, and L. Gao, “Deloading power coordinated distribution method for frequency regulation by wind farms considering wind speed differences”, *IEEE Access*, vol. 7, pp. 122573–122582, 2019.
- [28] A.I. Nusaif and A.L. Mahmood, “MPPT Algorithms (PSO, FA, and MFA) for PV System Under Partial Shading Condition, Case Study: BTS in Algalalia, Baghdad”, *International Journal of Smart Grid-ijSmartGrid*, vol. 4, no. 3, pp. 100–110, 2020.
- [29] S.F. Jaber, and A. M. Shakir, “Design and Simulation of a Boost-Microinverter for Optimized Photovoltaic System Performance”, *International Journal of Smart Grid-ijSmartGrid*, vol. 5, no. 2, pp. 94–102, 2021.